AIChE

Robust Fault Detection and Monitoring of Hybrid Process Systems with Uncertain Mode Transitions

Ye Hu and Nael H. El-Farra
Dept. of Chemical Engineering and Materials Science, University of California, Davis, CA 95616

DOI 10.1002/aic.12473
Published online December 28, 2010 in Wiley Online Library (wileyonlinelibrary.com).

A methodology for fault detection and monitoring of a class of hybrid process systems modeled by switched nonlinear systems with control actuator faults, uncertain continuous dynamics, and uncertain mode transitions is presented. A robust hybrid monitoring scheme that distinguishes reliably between faults, mode transitions, and uncertainty is developed using tools from unknown input observer theory and results from Lyapunov stability theory. The monitoring scheme consists of (1) a family of dedicated mode observers that locate the active operating mode at any given time and detect mode switches, (2) a family of robust Lyapunov-based fault detection schemes that detect the faults within the continuous modes, and (3) a supervisor that synchronizes the switching between different controllers and different fault detectors as the process transitions from one mode to another. A key idea of the developed framework is to design the mode observers in a way that facilitates the identification of the active mode without information from the controllers and renders the residuals insensitive to the faults and uncertainties in the constituent subsystems. The implementation of the developed monitoring scheme is demonstrated using a simulated model of a chemical reactor that switches between multiple operating modes. © 2010 American Institute of Chemical Engineers *AIChE J,* 57: 2783–2794, 2011

Keywords: fault detection, monitoring, uncertain mode transitions, hybrid process systems, model uncertainty, chemical processes

Introduction

Safety and reliability are primary concerns in the operation of chemical processes. The continued increase in the size and complexity of modern industrial plants, together with the increased reliance on automation, poses challenges in meeting these objectives because of the increased likelihood of faults, such as malfunctions in process equipment and failures of control instrumentation, which can undermine the stability and integrity of the entire system if not detected and handled appropriately. Not surprisingly, the problems of on-line fault detection and handling in dynamic process systems have been the subject of considerable research interest over the past few decades in both the academic and industrial circles in process control (for example, see[1–9] for some results and references in this area).

An examination of the existing literature on fault detection, however, shows that the majority of existing methods have been developed for purely continuous processes. Yet, many chemical processes are characterized by strong interactions between continuous dynamics and discrete events and are more appropriately modeled by hybrid systems. The distinguishing feature of a hybrid system is its multimodal structure characterized by switching between a finite number of continuous dynamical modes or subsystems. The continuous dynamics often arise from the underlying physical laws,

Correspondence concerning this article should be addressed to N. H. El-Farra at nhelfarra@ucdavis.edu.

such as mass, momentum, and energy conservation, and are typically modeled by continuous-time differential equations. The discrete events, on the other hand, can be the result of inherent physicochemical discontinuities in the continuous dynamics, transitions between different operating regimes, the use of discrete actuators and sensors in the control system, or the use of logic-based switching for supervisory and safety control.

The theoretical challenges posed by the combined discrete-continuous interactions, together with the abundance of practical application areas where such interactions arise, have motivated significant research work on the modeling and simulation,[10,11] optimization,[12] stability analysis,[13–16] and control[17,18] of various classes of hybrid systems. More recently, the fusion of hybrid system tools with advances in nonlinear process control has led to the formulation and solution of several control problems for nonlinear hybrid systems.[19–22] Research on this front has focused mainly on hybrid systems where a plant supervisor tries to verify or enforce a prescribed switching schedule to satisfy a higher operational objective. For this purpose, some form of *a priori* (though not necessarily exact) knowledge of mode transitions is assumed in the problem formulation. Compared with the efforts on the analysis and control of hybrid systems, however, the problems of fault detection and monitoring have received less attention. Examples of important contributions in this direction include the design of switched state estimation schemes for switched linear systems[23–25] as well as the development of fault diagnosis algorithms using hybrid automata theory,[26] hybrid bond graph models,[27,28] and statistical data-based methods.[29]

A key consideration in the design of model-based fault detection schemes for hybrid systems is the ability to discriminate effectively between process and/or control system faults on the one hand and the discrete transitions that take place between the continuous modes on the other. Failure to distinguish between faults and mode transitions can lead to false or missed alarms and subsequent instability or deterioration in the overall process performance. The monitoring problem for hybrid systems is further complicated by the presence of uncertainty in both the continuous dynamics and the discrete events governing the transitions between them. Uncertainty in the continuous dynamics arises typically because of the presence of unknown or partially known process parameters as well as time-varying exogenous disturbances, which if not properly accounted for can adversely affect the implementation of the monitoring and control systems. Uncertainty in the mode transitions, on the other hand, stems from the lack of *a priori* knowledge of either the timing or the sequence of transitions between the constituent modes. For example, in processes undergoing autonomous transitions, the timing and sequence of switches are determined by the evolution of the process and cannot be determined beforehand. For processes with controlled transitions, unexpected disruptions in raw material supplies and energy sources often force plant operation to deviate from the nominal schedule to minimize production losses and maintain the overall plant objectives. Beyond its impact on the detectability of faults, the uncertainty about when and how mode transitions take place can also have a detrimental effect on the ability of the supervisor to activate the appropriate controller at the right time, thus possibly leading to instability or performance deterioration. An effective hybrid monitoring scheme must, therefore, be robust with respect to such uncertainty and have the ability to decouple the effects of faults from mode transitions and disturbances.

Motivated by these considerations, we develop in this work a model-based architecture for monitoring and fault detection of uncertain nonlinear hybrid process systems subject to control actuator faults. The architecture consists of (1) a family of dedicated mode observers that are designed to identify the active mode at any given time and detect possible mode transitions, (2) a set of robust fault detectors that detect the actuator faults within the uncertain continuous modes, and (3) a supervisor that activates the corresponding controller and fault detector as the process transitions from one mode to another. The key idea is to design the mode observers in a way so that they are able to reliably detect mode transitions irrespective of faults and uncertainties in the system and without the aid of the controllers.

The rest of this article is organized as follows. Following some mathematical preliminaries, the hybrid monitoring problem is formulated and an overview of its solution is presented. A family of feedback controllers are then synthesized using Lyapunov-based control techniques to robustly stabilize the constituent modes in the absence of faults. The model-based monitoring structure is presented in the following section. To identify the active mode and detect transitions between different modes, a bank of dedicated mode observers that replicate the expected behavior of each mode are designed and run in parallel with the process for all times. Using ideas from unknown input observer theory, the observers are designed such that the residual of the observer for the active mode is decoupled from the faults and uncertainties, and thus is sensitive only to mode transitions. Analyzing the pattern of residuals then allows timely identification of the active mode and detection of mode transitions. Once a mode transition is detected and the new active mode is identified, the supervisor switches to the corresponding controller and fault detector to stabilize the process and monitor the operational health status of the control actuators within the active mode. An alarm threshold based on the expected fault-free behavior of each closed-loop subsystem is used for fault detection. Finally, the proposed theoretical framework is illustrated using a chemical process example.

Preliminaries

Class of systems

We consider switched uncertain nonlinear systems described by the following state-space representation

$$\begin{aligned} &\dot{x}(t) = A_i x(t) + f_i(x(t)) + B_i(u_i(t) + f_{ai}(t)) + W_i(x(t))\theta_i(t) \\ &y(t) = Cx(t),\ i(t) \in \mathcal{I} = \{1, 2, \cdots, N\} \\ &t^k_{i,\,\text{in}} \le t \le t^k_{i,\,\text{out}},\ k \in \{1, 2, \cdots\} \end{aligned} \tag{1}$$

where $x \in \mathbb{R}^n$ denotes the vector of continuous-time state variables, $u_i = [u_i^1 \ \ldots \ u_i^m]^T \in \mathbb{R}^m$ denotes the vector of continuous manipulated inputs associated with the i-th mode, f_{ai} denotes a fault in the control actuators of the i-th mode, $\theta_i(t) = [\theta_i^1(t) \ \ldots \ \theta_i^q(t)]^T \in \Theta_i \subset \mathbb{R}^q$ denotes the vector of uncertain

(possibly time-varying) but bounded variables that takes values in a nonempty compact convex subset of $\mathbb{R}^q$ and describes parametric uncertainty and/or time-varying external disturbances, and $y \in \mathbb{R}^p$ denotes the vector of output variables. A_i, B_i, $W_i(\cdot)$, and C are $n \times n$, $n \times m$, $n \times q$, and $p \times n$ matrices, respectively. f_i: $\mathbb{D} \to \mathbb{R}^n$ denotes a Lipschitz map and $\mathbb{D} \subset \mathbb{R}^n$ is a domain that contains the origin $x = 0$. The switching signal i:$[0, \infty) \to \mathcal{I}$ is assumed to be a piecewise continuous (from the right) function of time, i.e., $i(t^k) = \lim_{t \to t^{k+}} i(t)$ for all k, implying that only a finite number of switches are allowed on any finite interval of time. The variable i, which takes values in the finite index set $\mathcal{I}$, represents a discrete state that indexes the matrices A_i, B_i, $W_i(\cdot)$, the vector field $f_i(\cdot)$, the control input u_i, the actuator fault f_{ai}, and the uncertain variable θ_i, which altogether determine $\dot{x}$. It is assumed that all entries of the vector field $f_i(\cdot)$ and the $n \times q$ matrix $W_i(\cdot)$ are sufficiently smooth. We also assume that the continuous-time state variable, x, does not jump when the system switches between modes, which means that x is everywhere continuous. The notations $t^k_{i,\text{in}}$ and $t^k_{i,\text{out}}$ are used to denote the k-th time that the i-th mode is switched in and out, respectively. During the time period that the i-th mode is active, the temporal evolution of x is governed by the set of differential equations indexed by i.

As the system described by Eq. 1 consists of a finite number of different modes, it is usually referred to as multimodal or a variable structure system. Triggered by some discrete events, which can either be dependent on the process itself (i.e., autonomous) or controlled by some high-level supervisor, the system switches between its constituent modes. Note that although the quasi-linear structure of the hybrid system of Eq. 1 is considered for convenience to simplify the analysis and design tasks, this structure is quite common in many practical systems such as chemical processes in which material and energy flows (which usually depend linearly on the state variables) are coupled with chemical reactions (whose rates typically depend nonlinearly on the state variables).

Problem formulation and solution overview

Referring to the system of Eq. 1 where at any time only one of the N modes is active, the problems under consideration include how to robustly stabilize the constituent subsystems under uncertainty, how to identify which subsystem is active at any given time, and how to determine the fault or health status of the control actuators within the active mode. To address these problems, we consider the following integrated control and monitoring approach:

1. Synthesize, for each mode, a robustly stabilizing feedback controller and obtain an explicit characterization of the fault-free behavior of each mode in terms of a time-varying bound on the state.

2. Design a bank of dedicated mode observers to ensure timely identification of the active mode and detection of the transitions between modes. As faults, uncertainties, and mode transitions all influence the process dynamics, the mode observer for the active mode should be designed so that its residual is completely decoupled from faults and uncertainties and is sensitive only to mode transitions. Once the active mode is identified, the corresponding controller should be activated.

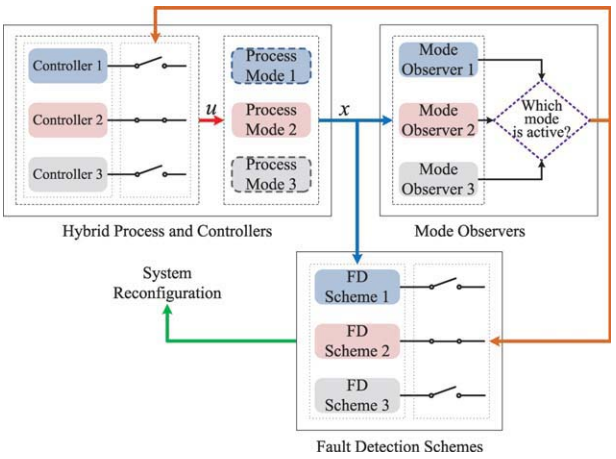

Figure 1. Overview of the hybrid monitoring structure.

[Color figure can be viewed in the online issue, which is available at wileyonlinelibrary.com.]

3. Develop a fault detection scheme for each continuous mode by using the fault-free bound established in step 1 as an alarm threshold. Once the active mode is identified, the corresponding fault detection scheme should be activated.

Figure 1 is a schematic depiction of the different layers in the hierarchical hybrid monitoring structure for a switched uncertain system with three modes where a controller has been designed for each mode. As can be seen from the figure, all mode observers receive state information from the process and run in parallel for all times. The identification of the active mode is based on evaluating the residuals generated by the observers, which capture the differences between the process state and the outputs of the observers. After the active mode is identified, the corresponding controller and fault detector are activated to stabilize the plant and determine whether an actuator fault exists within the active mode. The next two sections provide a detailed description of the design and implementation of the proposed hybrid monitoring structure.

Robust Feedback Controller Synthesis

Consider the switched nonlinear system of Eq. 1 and, without loss of generality, assume that the uncertain variables are nonvanishing (i.e., the nominal equilibrium point for each mode is no longer an equilibrium point of the uncertain subsystem) and are bounded by $\|\theta_i\| \leq \theta_{bi}$, where $\|\cdot\|$ denotes the Euclidean norm of a vector or matrix. Using a robust control Lyapunov function $V_i(x)$: $\mathbb{R}^n \to \mathbb{R}^+$ for each mode, the following robust nonlinear controller can be designed using the results in.[22,30–32]

$$u_i = -k_i(x, \theta_{bi}, \chi_i, \phi_i)(L_{B_i} V_i)^T, \; i \in \mathcal{I} \tag{2}$$

where

$$k_i(\cdot) = \begin{cases} \dfrac{\alpha_i(x) + \sqrt{(\alpha_i^*(x))^2 + (\beta_i(x))^4}}{(\beta_i(x))^2}, & \beta_i(x) \neq 0 \\ 0, & \beta_i(x) = 0 \end{cases} \tag{3}$$

$$\alpha_i = L_{\tilde{f}_i} V_i + (\rho_i \|x\| + \chi_i \theta_{bi} \|L_{W_i} V_i\|) \left(\frac{\|x\|}{\|x\| + \phi_i} \right) \quad (4)$$

$$\alpha_i^* = L_{\tilde{f}_i} V_i + \rho_i \|x\| + \chi_i \theta_{bi} \|L_{W_i} V_i\| \quad (5)$$

$$\beta_i = \|(L_{B_i} V_i)^T\| \quad (6)$$

where $k_i(\cdot)$ is a nonlinear scalar gain designed so that the energy for the i-th mode — which is captured by V_i — decreases monotonically whenever the i-th mode is active, $L_{\tilde{f}_i} V_i$ is the Lie derivative of V_i with respect to $\tilde{f}_i(x) := A_i x + f_i(x)$, $L_{B_i} V_i$ and $L_{W_i} V_i$ are row vectors of the Lie derivatives of V_i with respect to the columns of B_i and $W_i(x)$, respectively, ρ_i, χ_i, and ϕ_i are tunable parameters that satisfy $\rho_i > 0$, $\chi_i > 1$, and $\phi_i > 0$. The following proposition establishes that the controller of Eqs. 2–6 enforces robust closed-loop stability for each mode with an arbitrary degree of attenuation of the effects of uncertainty and guarantees convergence to a small neighborhood of the nominal equilibrium point in finite time (see[19] for a similar proof).

Proposition 1. *Consider the closed-loop system of Eq. 1 with $f_{ai} \equiv 0$ for a given $i \in \mathcal{I}$ under the control law of Eqs. 2–6. Then, there exists a positive real number κ_i and a class $\mathcal{K}$ function[*] $\psi_i(\cdot)$ such that the time derivative of V_i along the trajectories of the closed-loop system satisfies*

$$\dot{V}_i(x(t)) \leq -\kappa_i V_i(x(t)) + \psi_i(\mu_i) \quad (7)$$

where $\mu_i = \phi_i(\chi_i - 1)^{-1}$. Furthermore, given any positive real number ϵ_i, there exists $\tilde{\mu}_i$ such that if $\mu_i \leq \tilde{\mu}_i$, $\limsup_{t\to\infty} V_i(x(t)) \leq \epsilon_i$ and the nominal equilibrium point of the system is practically stable.

Remark 1. It should be noted that while Lyapunov-based control techniques have been used to synthesize the robust feedback control laws, this choice is not unique and any other control law capable of robustly stabilizing the constituent modes and the overall switched system can be used instead. An advantage of Lyapunov-based control methods is that by designing each controller to shape the time derivative of the Lyapunov function, an explicit characterization of the expected fault-free evolution of each mode can be obtained in terms of a time-varying bound that depends on the state and the controller tuning parameters. This controller-induced feature will facilitate the design and implementation of a robust fault detection scheme for each mode.

Remark 2. For switched systems with only a finite number of mode transitions, robust stabilization of the continuous modes is sufficient to guarantee stability of the overall system. However, when considering an infinite number of mode transitions over the infinite time interval, additional restrictions on the growth of each Lyapunov function for the time periods during which the corresponding mode is inactive are needed. This is typically expressed in the form of a multiple Lyapunov function (MLF) stability constraint.[13] An example is to require $V_i(x(t_{i,\text{out}}^{k+1})) < V_i(x(t_{i,\text{out}}^k))$ for $V_i > \epsilon_i$. Assuming a minimum dwell time for each mode, $t_{i,\text{out}}^k - t_{i,\text{in}}^k \geq \Delta_i$, this MLF stability condition can be enforced by appropriately adjusting the tuning parameters of the i-th controller every time that the i-th mode is activated to ensure an appropriate decay rate for V_i.

Design of Hybrid Monitoring and Fault Detection Schemes

Having designed a stabilizing controller for each mode, the supervisor needs to identify which mode is active at any given time in order to: (1) activate the corresponding controller and ensure synchronous process/controller transitions and (2) activate the corresponding fault detection scheme.

Mode identification and mode transition detection

To replicate the expected dynamic behavior of each continuous mode in the switched system of Eq. 1 and be able to distinguish mode transitions from faults and uncertainties, we construct the following set of state observers (inspired by the ideas in[6] and[33])

$$\begin{aligned} \dot{\eta}_i &= L_i \eta_i + K_i y + (I - H_i C) f_i(\xi_i) \\ \xi_i &= \eta_i + H_i y, \; r_i = x - \xi_i, \; i \in \mathcal{I} \end{aligned} \quad (8)$$

where $\eta_i \in \mathbb{R}^n$ denotes the vector of states for the i-th observer, $\xi_i \in \mathbb{R}^n$ denotes the vector of observer outputs, $r_i \in \mathbb{R}^n$ is the vector of residuals defined as the differences between the actual states of the process and the observer outputs, and y is the process output. The matrix I is the identity matrix, and matrices L_i, K_i and H_i are design parameters. The following theorem summarizes how the mode observers of Eq. 8 are designed to allow timely identification of the active mode and detection of mode transitions irrespective of faults and uncertainties in the constituent subsystems. The proof of this theorem is given in Appendix A.

Theorem 1. *Consider the switched uncertain nonlinear system of Eq. 1 and the family of mode observers in Eq. 8 where the matrices L_i, H_i, and K_i are chosen such that the following relations hold*

$$(I - H_i C) A_i - L_i (I - H_i C) - K_i C = 0 \quad (9)$$

$$(I - H_i C) B_i = 0 \quad (10)$$

$$(I - H_i C) W_i(x) = 0 \quad (11)$$

$$I - H_i C \neq 0 \quad (12)$$

Without loss of generality, let mode ε, for some $\varepsilon \in \mathcal{I}$, be the active one. Then, the evolution of residual r_ε is governed by

$$\dot{r}_\varepsilon = L_\varepsilon r_\varepsilon + (I - H_\varepsilon C)[f_\varepsilon(x) - f_\varepsilon(\xi_\varepsilon)] \quad (13)$$

And the residuals for the inactive modes, $j \in \mathcal{I} - \{\varepsilon\}$, obey the following dynamics

$$\begin{aligned} \dot{r}_j =& L_j r_j + (I - H_j C)[(A_\varepsilon - A_j)x + f_\varepsilon(x) - f_j(\xi_j)] \\ &+ (I - H_j C)[B_\varepsilon(u_\varepsilon + f_{a\varepsilon}) + W_\varepsilon(x)\theta_\varepsilon] \end{aligned} \quad (14)$$

The stability property of the zero equilibrium point of Eq. 13 is discussed in the following proposition and its proof is given in Appendix B.

Proposition 2. *Consider the system of Eq. 13 where the matrix L_ε is chosen to be Hurwitz and $f_\varepsilon(\cdot)$ is Lipschitz on*

[*] A function $\psi(\cdot)$ is said to be of class $\mathcal{K}$ if it is strictly increasing and $\psi(0) = 0$.

some domain $\mathbb{D} \subset \mathbb{R}^n$ *(i.e., there exists a positive constant* ω_ε *such that, for all* $x \in \mathbb{D}$ *and* $\xi_\varepsilon \in \mathbb{D}$, $\|f_\varepsilon(x) - f_\varepsilon(\xi_\varepsilon)\| \leq \omega_\varepsilon \| x - \xi_\varepsilon\|$*. Then, the origin* $r_\varepsilon = 0$ *is asymptotically stable*

Remark 3. It can be seen from Eq. 14 that even if the matrix L_j is chosen to be Hurwitz, the residual r_j will not converge to the origin because the additive term $(I - H_jC)[(A_\varepsilon - A_j)x + f_\varepsilon(x) - f_j(\xi_j) + B_\varepsilon(u_\varepsilon + f_{a\varepsilon}) + W_\varepsilon(x)\ \theta_\varepsilon]$ is in general nonzero and nonvanishing, and thus the origin is no longer the equilibrium point for the system of Eq. 14. Therefore, although the residual for the active mode will converge to zero, the residuals for the inactive modes will exhibit offsets, and this serves as the criterion for identifying the active mode and detecting mode transitions. Specifically, whenever an active mode — say mode i — is switched out, the residual of the corresponding mode observer, $r_i(t)$, will no longer converge to zero and a nonzero offset will appear, which indicates that a mode transition has taken place and that the i-th mode is no longer active from then until $r_i(t)$ falls back to zero again. Note also that the decoupling conditions of Eqs. 9–12 ensure that only the residual corresponding to the active mode is insensitive to faults and uncertainties. Residuals corresponding to the inactive modes, however, will in general be influenced by the faults and uncertainties in the active mode as their dynamics are governed by Eq. 14.

Remark 4. The necessary conditions for Eqs. 10 and 11 to be solvable are $\text{rank}(CB_i) = \text{rank}(B_i)$ and $\text{rank}(CW_i(x)) = \text{rank}(W_i(x))$. These two equations imply that $\text{rank}(B_i) \leq \text{rank}(C)$ and $\text{rank}(W_i(x)) \leq \text{rank}(C)$, which means that if the residual evolution can be decoupled from the faults and uncertainties, the number of different channels where faults and uncertainties enter the system cannot be greater than the number of independent measurements the system has. If matrices B_i and $W_i(x)$ have full column ranks, we can further assert that the aforementioned necessary conditions are also sufficient for solvability. Another conclusion that can be drawn from the necessary conditions for solvability is that the conditions $\dim \text{Ker}(C) \cap \text{Im}(B_i) = 0$ and $\dim \text{Ker}(C) \cap \text{Im}(W_i(x)) = 0$, where $\text{Ker}(\cdot)$ and $\text{Im}(\cdot)$ denote the kernel and image of a matrix, respectively, must hold. In addition to Eqs. 10 and 11, Eq. 12 also has to be satisfied, which poses one more constraint on B_i and $W_i(x)$, specifically $\text{rank}(B_i) \leq n - 1$ and $\text{rank}(W_i(x)) \leq n - 1$. Note that Eq. 11 must be satisfied for all x so that uncertainty can always be decoupled from the residual for the active mode. Restrictive as this constraint may seem, a matrix C that has full column rank ensures that $W_i(x)$ satisfies the requirement $\dim \text{Ker}(C) \cap \text{Im}(W_i(x)) = 0$ unconditionally since $\text{Ker}(C) = 0$; moreover, $W_i(x)$ usually exhibits a certain structure in terms of the locations of the zeros, and as long as the structure guarantees $\dim \text{Ker}(C) \cap \text{Im}(W_i(x)) = 0$ and $\text{rank}(W_i(x)) \leq n - 1$, and remains unvaried, changes in the values of the state-dependent elements of $W_i(x)$ due to the evolution of x will not influence the satisfaction of these conditions. For example, in the chemical reactor model considered in the simulation section, C is a 2×2 identity matrix, and $W_i(x)$ is a 2×2 matrix whose first row consists entirely of zeros, whereas the elements of the second row vary with x (uncertainty is considered only in the feed temperature and heats of reaction). Based on this structure, it can be verified that both of the aforementioned conditions are always satisfied because $\text{Ker}(C) = 0$ and $\text{rank}(W_i(x)) = 1$.

Remark 5. The choices for L_i and K_i are constrained by Eq. 9, which is essentially a Sylvester equation. To gain some insight into the implications of this condition, let us assume, for simplicity, that $I - H_iC$ has full rank, and thus

$$L_i = (I - H_iC)A_i(I - H_iC)^{-1} - K_iC(I - H_iC)^{-1}$$

The eigenvalues of L_i can be arbitrarily placed in the open left half of the complex plane via K_i if and only if the pair $(\overline{C}_i, \overline{A}_i)$ is at least detectable, where

$$\bar{C}_i = C(I - H_iC)^{-1}, \quad \overline{A}_i = (I - H_iC)A_i(I - H_iC)^{-1}$$

If the matrix $I - H_iC$ is rank deficient, the solvability of Eq. 9 might be difficult to analyze. In consideration of this, when the proposed mode observers are implemented in practice, the matrices H_i should be chosen first such that Eqs. 10–12 are satisfied. Then, the set of Hurwitz matrices L_i are selected and they, as well as H_i, are substituted into Eq. 9 to calculate the desired matrices K_i.

Remark 6. In addition to the mode observers considered in Eq. 8, one could design the following set of mode observers as an alternative approach for solving the mode identification and mode transition detection problems

$$\dot{\eta}_i = L_i\eta_i + K_iy + f_i(\eta_i),\ r_i = y - C\eta_i,\ i\ \in \mathcal{I}$$

where only the output of the process, y, is used to evaluate the residual. This design approach, however, introduces a number of important limitations and is more restrictive than the one proposed in Eq. 8. For example, calculating the governing equation for the evolution of the residual defined in the above equation requires expressing η_i in terms of r_i and y using the definition of the residual, which incurs the left inverse of the output matrix C that may not exist if C is rank deficient. Moreover, to decouple the residual for the active mode from the control input, the actuator fault, and the uncertainty, the matrices of the system and the mode observer would have to satisfy much more restrictive conditions; for example, $CB_i = 0$ must hold to render the residual r_i insensitive to the control input as well as the actuator fault, and this condition implies that $\text{rank}(B_i) + \text{rank}(C) \leq n$, which is not satisfied for the chemical reactor model considered in the simulation example.

Fault detection within the constituent modes

In this subsection, we describe how the characteristic closed-loop behavior obtained in the controller synthesis section for each fault-free subsystem can be used as the basis for deriving rules for fault detection within each mode. The key idea is to use the time-varying bound on $\dot{V}_i$ established in Eq. 7 as a dedicated alarm threshold that determines the fault or health status of the actuators within the i-th mode. By monitoring the evolution of the closed-loop state, a fault can be declared if the corresponding alarm threshold is breached. These ideas are formalized in the following proposition. The proof follows from Proposition 1 and is omitted for brevity.

Proposition 3. *Consider the closed-loop system of Eq. 1 under the control law of Eqs. 2–6, for a given* $i \in \mathcal{I}$*, and let* $\epsilon_i := \frac{2\psi_i(\mu_i)}{\kappa_i}$*, where* κ_i*,* ψ_i*, and* μ_i *were defined in Proposition*

1. If, at some time $T > 0$, either: (a) $\dot{V}_i(x(T)) > -\frac{\kappa_i}{2}V_i(x(T))$ where $V_i(x(T^-)) > \epsilon_i$ or (b) $V_i(x(T)) > \epsilon_i$ where $V_i(x(T^-)) \leq \epsilon_i$, then $f_{ai}(T) \neq 0$ and an actuator fault in the i*-th mode is declared*

Remark 7. The first condition (a) in Proposition 3 provides the detection rule for the case when, immediately prior to the fault, the state lies outside the terminal set. In this case, a fault that causes an increase in V_i (destabilizing fault) as well as a fault that slows down the decay of V_i beyond the minimum rate enforced by the healthy controller (performance-degrading fault) will be detected. The second condition (b) gives the rule for the case when, immediately prior to the fault, the state is already within the terminal set. In this case, a fault that causes the state to begin to escape the terminal set gets detected (recall from Proposition 1 that in the absence of faults the state is expected to remain confined within the terminal set once inside). Essentially, this approach uses the time derivative of the Lyapunov function of each mode as a residual and compares it against a time-varying threshold. Note that the set of faults that can be detected using this approach consists of all faults that breach the thresholds in Proposition 3. Any fault outside this set (i.e., a fault that does not cause a breach) will go undetected. Such faults, however, are not detrimental to the stability and performance of the process and thus require no corrective action.

Remark 8. Note that the alarm thresholds for fault detection can be tightened through proper selection of the controllers' tuning parameters. Specifically, by choosing a smaller ϕ_i and/or a larger χ_i, $\mu_i = \phi_i/(\chi_i - 1)$ can be made smaller, and this leads to a smaller ϵ_i as $\psi_i(\cdot)$ is a class $\mathcal{K}$ function of its argument. This choice of controller tuning parameters ensures that, in the absence of faults, the controller drives the state to converge to a smaller neighborhood of the nominal equilibrium point. The alarm threshold can also be tightened by choosing a larger ρ_i and/or a smaller ϕ_i, which lead to a larger κ_i, i.e., a faster rate of decay of the Lyapunov function in the absence of faults. These properties can be used to ensure timely fault detection and enhance the ability of the control system to recover from faults through actuator reconfiguration as well as to robustly stabilize the system in the absence of faults. Note also that the fault detection scheme presented in Proposition 3 can be used to detect both incipient and abrupt actuator faults, multiple simultaneous faults, and faults that do not necessarily appear in the actuators, as long as they influence the evolution of the states.

Remark 9. Unlike the mode observers, which run continuously and in parallel to the process, the fault detection scheme for a given mode is activated by the supervisor only when a determination is made (based on the residuals of the mode observers) that this mode is active.

Remark 10. Referring to the system of Eq. 1, an alternative approach for fault detection is to construct a switched fault detection filter of the following form using unknown input observer theory

$$\begin{aligned} \dot{z} &= M_i z + G_i B_i u + J_i y + (I - E_i C) f_i(\zeta_i) \\ \zeta_i &= z + E_i y,\ e = x - \zeta_i,\ i \in \mathcal{I} \end{aligned} \tag{15}$$

where $z \in \mathbb{R}^n$ denotes the vector of states of the filter, $\zeta_i \in \mathbb{R}^n$ denotes the vector of filter outputs, $e \in \mathbb{R}^n$ is the vector of residual signals, and M_i, G_i, J_i, and E_i are constant design matrices. If M_i is chosen to be Hurwitz and G_i, J_i, and E_i are selected such that

$$(I - E_i C)A_i - M_i(I - E_i C) - J_i C = 0 \tag{16}$$

$$[(I - E_i C) - G_i]B_i = 0 \tag{17}$$

$$(I - E_i C)W_i(x) = 0 \tag{18}$$

$$(I - E_i C)B_i \neq 0 \tag{19}$$

then, assuming that mode ε is active for some $\varepsilon \in \mathcal{I}$, the evolution of residual e is governed by

$$\dot{e} = M_\varepsilon e + (I - E_\varepsilon C)B_\varepsilon f_{a\varepsilon} + (I - E_\varepsilon C)[f_\varepsilon(x) - f_\varepsilon(\zeta_\varepsilon)]$$

As can be seen from the above equation, the evolution of the residual becomes decoupled from the uncertain variables. The stability properties of the residual with (or without) a fault are similar to those of Eq. 14 (or Eq. 13) (the proof is omitted here for brevity). An additional consideration in the design of this observer-based fault detection filter is the need to ensure residual convergence under switching. As the fault detection filter of Eq. 15 is itself a hybrid system, restrictions must be placed on the design matrices to ensure stability and convergence in the absence of faults. This can typically be addressed using either a common Lyapunov function or multiple Lyapunov functions approach.

Simulation Study: Application to a Chemical Reactor with Multiple Operating Modes

In this section, we present a simulation study that illustrates the application of the developed hybrid monitoring methodology to a hybrid nonlinear chemical process subject to model uncertainties and actuator faults. To this end, we consider a well-mixed, nonisothermal continuous stirred tank reactor where an irreversible elementary exothermic reaction of the form $A \xrightarrow{k_0} B$ takes place, with A being the reactant species and B the desired product.

As shown in Figure 2, the reactor can operate in one of three modes. In mode 1, the reactor has only one inlet stream containing fresh A at flow rate F_1, molar concentration C_{A1}, and temperature T_{A1}. In mode 2, another feed stream providing species A at flow rate F_2, molar concentration C_{A2}, and temperature T_{A2} is added. In mode 3, one additional stream feeding pure A at flow rate F_3, molar concentration C_{A3}, and temperature T_{A3} is introduced. When the operating requirements change (for example, when a higher yield is desired), a mode transition is triggered. Because of the nonisothermal nature of the reaction, a jacket is used to remove or provide heat to the reactor. Under standard modeling assumptions, a hybrid model of the following form can be derived from material and energy balance

$$\begin{aligned} \dot{C}_A &= \sum_{l=1}^{3} \sigma_l(t)\frac{F_l}{V}(C_{Al} - C_A) - r(C_A, T) \\ \dot{T} &= \sum_{l=1}^{3} \sigma_l(t)\frac{F_l}{V}(T_{Al} - T) + \frac{-\Delta H_r}{\rho c_p} r(C_A, T) + \frac{Q}{\rho c_p V} \end{aligned} \tag{20}$$

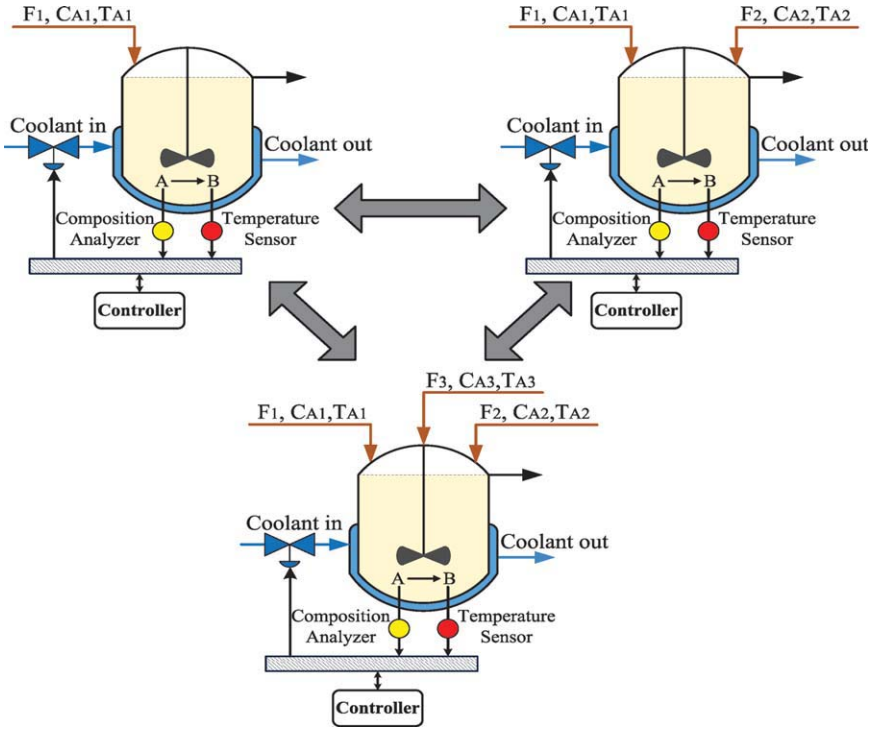

Figure 2. A switched nonisothermal continuous stirred tank reactor.

[Color figure can be viewed in the online issue, which is available at wileyonlinelibrary.com.]

where $r(C_A,T) = k_0 \exp\left(\frac{-E}{RT}\right)C_A$, C_A denotes the concentration of species A, T denotes the temperature of the reactor, l is the index for feed stream, $\sigma_l(t)$ can either be 0 or 1, representing the removal or addition of a new feed stream, V is the volume of the reactor, k_0, E, ΔH_r are the pre-exponential constant, the activation energy, and the enthalpy of the reaction, R is the gas constant, c_p and ρ are the heat capacity and density of the fluid in the reactor, and Q is the rate of heat input to the reactor.

Table 1. Process Parameters and Steady–State Values for the Chemical Reactor in Figure 2

$F_1 = 4.998\ m^3/h$
$F_2 = 12.998\ m^3/h$
$F_3 = 16.998\ m^3/h$
$C_{A1} = 4.0\ kmol/m^3$
$C_{A2} = 4.5\ kmol/m^3$
$C_{A3} = 5.0\ kmol/m^3$
$T_{A1} = 295.0\ K$
$T_{A2} = 320.0\ K$
$T_{A3} = 340.0\ K$
$T_{A1}^{nom} = 300.0\ K$
$Q_1^{nom} = 0\ kJ/h$
$Q_2^{nom} = 187{,}768\ kJ/h$
$Q_3^{nom} = 367{,}978\ kJ/h$
$V = 1.0\ m^3$
$R = 8.314\ kJ/kmol \cdot K$
$\Delta H_r^{nom} = -5.0 \times 10^4\ kJ/kmol$
$k_0 = 3.0 \times 10^6\ h^{-1}$
$E = 5.0 \times 10^4\ kJ/kmol$
$\rho = 1000.0\ kg/m^3$
$c_p = 0.231\ kJ/kg \cdot K$
$C_{A1}^s = 3.59\ kmol/m^3$
$C_{A2}^s = 4.23\ kmol/m^3$
$C_{A3}^s = 4.60\ kmol/m^3$
$T^s = 388.57\ K$

Using typical values for the process parameters (see Table 1), the reactor with $Q = Q_i^{nom}$ (Q_i^{nom} is the nominal value of the heat input rate for the i-th mode) usually has three equilibrium points for the i-th mode: two locally asymptotically stable and one unstable. The control objective here is to stabilize each mode at its unstable equilibrium point $(C_A^{1s}, T^s) = (3.59\ kmol/m^3, 388.57\ K)$, $(C_A^{2s}, T^s) = (4.23\ kmol/m^3, 388.57\ K)$, and $(C_A^{3s}, T^s) = (4.60\ kmol/m^3, 388.57\ K)$ in the presence of parametric uncertainty in the enthalpy of the reaction (this uncertainty is simulated by time-varying white noise bounded by 10 kJ/kmol with an average of ΔH_r^{nom}) and in the temperature for the first feed stream T_{A1} (which is chosen 5 K lower than the value used for controller synthesis). Operation at the unstable equilibrium points is intended to avoid high reactor temperature while achieving reasonable conversion. The manipulated input used is the rate of heat input (see Figure 2), $u_i = Q - Q_i^{nom}$. Measurements of the temperature and concentration are assumed to be available. We define the displacement variables $x = [x_1\ x_2]^T = [C_A - C_A^{1s}\ T - T^s]^T$ so that the equilibrium point for the first mode x_1^s is placed at the origin. With this definition, the equilibrium points for the second and third modes are also shifted to $x_2^s = [0.64\ 0]^T$ and $x_3^s = [1.01\ 0]^T$, respectively, (units for state variables are dropped).

Following the methodology presented in the controller synthesis section, a Lyapunov function of the form $V_i(x) = \|x - x_i^s\|^2$, $i \in \{1,2,3\}$ is used to synthesize the Lyapunov-based controller for each mode. Note that as we consider only a finite number of mode transitions in this example, stability of each continuous closed-loop mode is sufficient to ensure stability of the overall switched system. In the simulation, the terminal set for each mode has been chosen as $\Omega_i = \{x \in \mathbb{R}^2 | V_i(x) \leq 2\}$ and the following tuning parameters

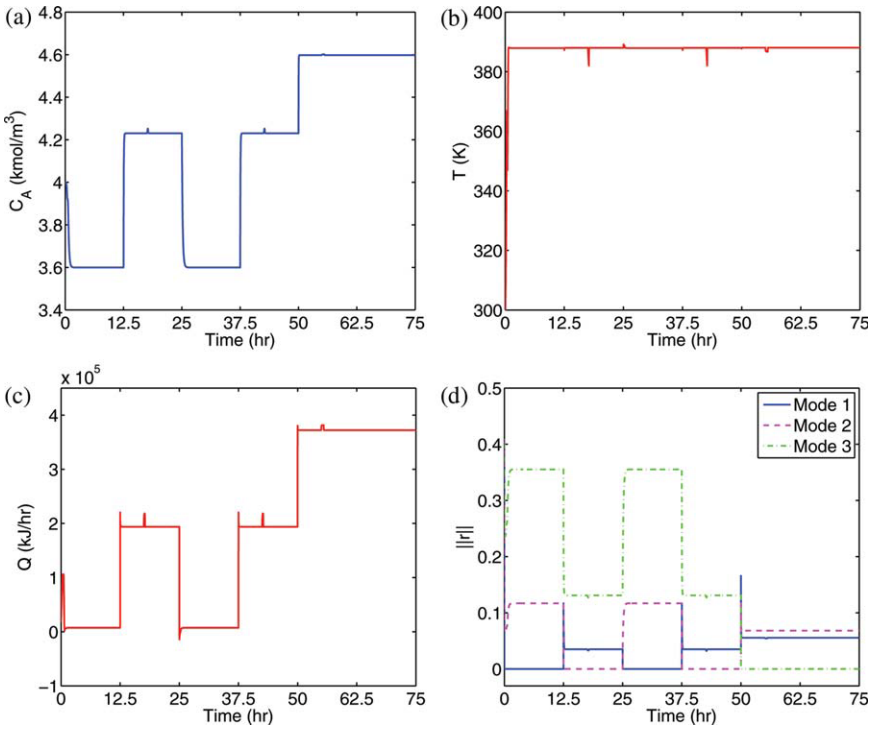

Figure 3. Evolution of the closed-loop reactant concentration (a), reactor temperature (b), rate of heat input (c), and residuals of the mode observers (d) as the reactor switches from mode 1 to mode 2 to mode 1 to mode 2 to mode 3 at $t = 12.5$, $t = 25$, $t = 37.5$, and $t = 50$ h, respectively.

[Color figure can be viewed in the online issue, which is available at wileyonlinelibrary.com.]

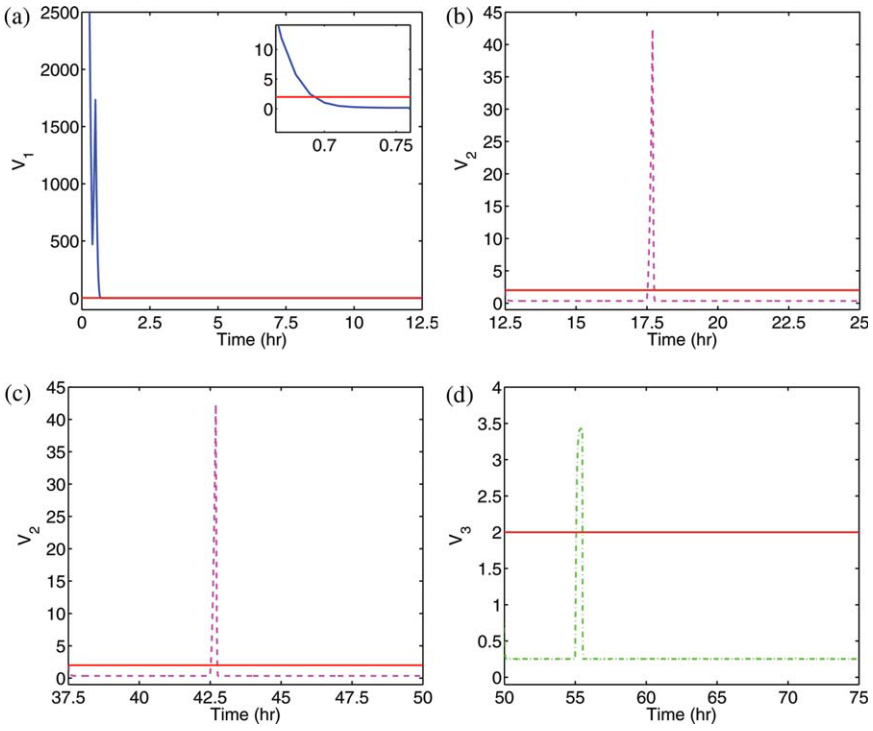

Figure 4. Evolution of the values of Lyapunov functions at the time of (a) the first fault (0.4–0.5 h), (b) the second fault (17.5–17.7 h), (c) the third fault (42.5–42.7 h), and (d) the fourth fault (55.0–55.5 h).

[Color figure can be viewed in the online issue, which is available at wileyonlinelibrary.com.]

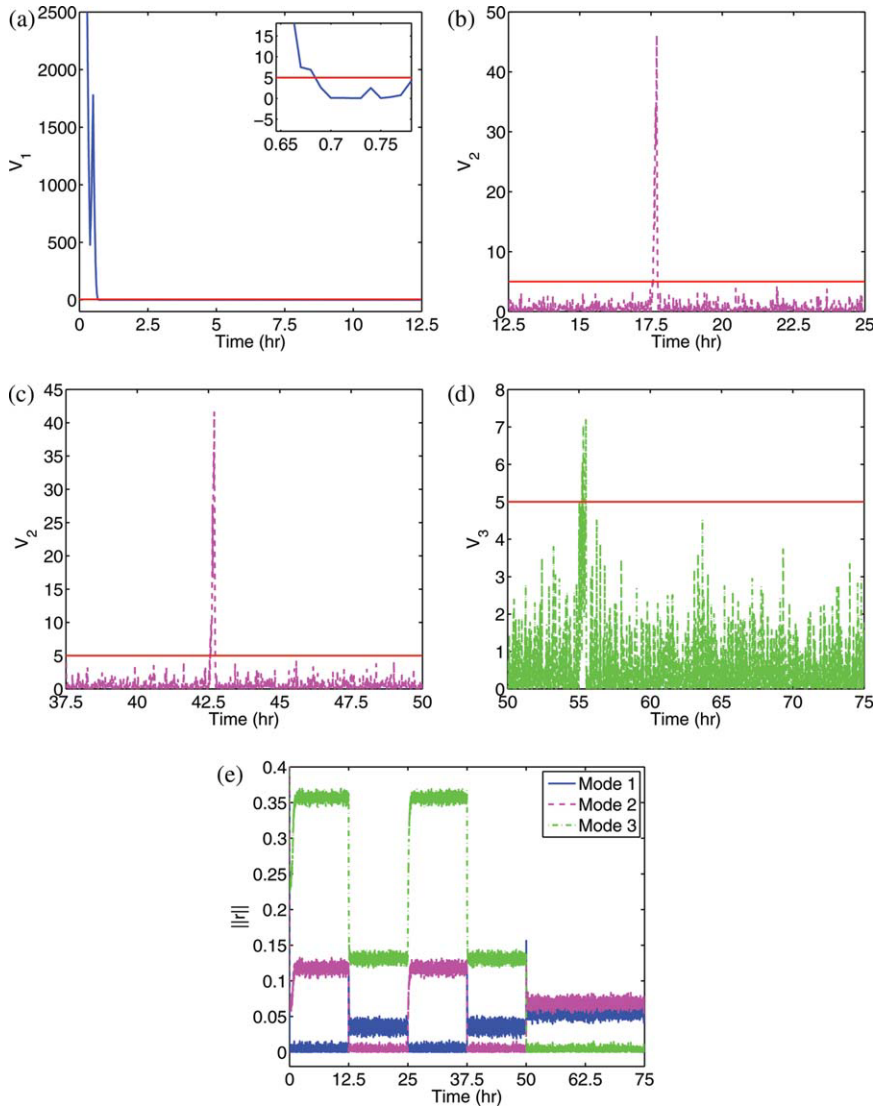

Figure 5. Evolution of the values of the Lyapunov functions at the time of (a) the first fault (0.4–0.5 h), (b) the second fault (17.5–17.7 h), (c) the third fault (42.5–42.7 h), and (d) the fourth fault (55.0–55.5 h) in the presence of measurement noise and (e) evolution of the residuals of the mode observers in the presence of measurement noise as the reactor switches from mode 1 to mode 2 to mode 1 to mode 2 to mode 3 at t = 12.5, t = 25, t = 37.5, and t = 50 h, respectively.

[Color figure can be viewed in the online issue, which is available at wileyonlinelibrary.com.]

are used: $\rho_i = 0.0005$, $\chi_i = 1.2$, and $\phi_i = 0.1$. Next, the mode observers of Eq. 8 are designed, where the matrices L_i, K_i, and H_i are chosen to satisfy the conditions of Eqs. 9–12

$$L_1 = L_2 = L_3 = \begin{bmatrix} -100 & 0 \\ 0 & -100 \end{bmatrix}$$

$$H_1 = H_2 = H_3 = \begin{bmatrix} 1 & 0 \\ 1 & 1 \end{bmatrix}$$

$$K_1 = \begin{bmatrix} 0 & 0 \\ -95.002 & 0 \end{bmatrix}, \quad K_2 = \begin{bmatrix} 0 & 0 \\ -82.004 & 0 \end{bmatrix},$$

$$K_3 = \begin{bmatrix} 0 & 0 \\ -65.006 & 0 \end{bmatrix}$$

To design the fault detection scheme for each mode, the robust control Lyapunov functions V_i are used to assess the stability and performance of the closed-loop subsystem, and a constant alarm threshold based on the size of the terminal set enforced in the absence of faults is used. For the case when $V_i(x(T^-)) > \epsilon_i$, a fault is declared whenever $\dot{V}_i(x(T)) > 0$. This is a less restrictive threshold than the one proposed in Proposition 3 as $\dot{V}_i(x(T)) > 0 \Rightarrow \dot{V}_i(x(T)) > -\frac{\kappa_i}{2} V_i(x(T))$. An advantage of using this threshold is that this condition can be verified by monitoring the value of the Lyapunov function V_i itself without explicitly calculating the time derivative of V_i. However, one could follow the criterion exactly as stated in Proposition 3 so that an actuator fault is declared when the rate of decay of the Lyapunov function decreases, but this makes little difference in this particular example. It should be noted

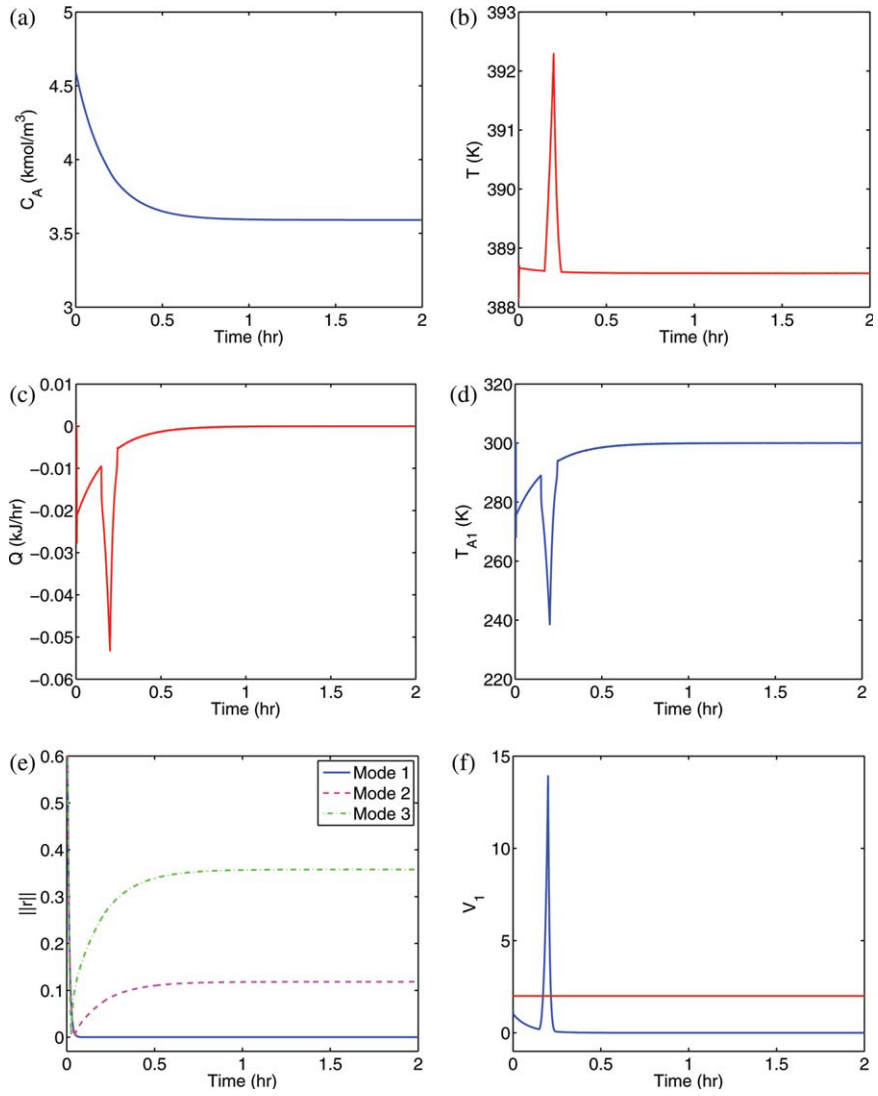

Figure 6. Evolution of the closed-loop reactant concentration (a), reactor temperature (b), rate of heat input (c), inlet temperature for the first feed stream (d), residuals of the mode observers (e), and the value of the Lyapunov function V_1 (f), when the reactor operates in mode 1 and is subject to multiple simultaneous faults in the control actuators.

[Color figure can be viewed in the online issue, which is available at wileyonlinelibrary.com.]

that the alternative approach for fault detection described in Remark 10 cannot be applied here. The reason is that Eqs. 18 and 19 cannot be satisfied simultaneously due to the fact that the column vectors of the matrix $W_i(x)$ are colinear with the input matrix B_i (which is actually a vector here) as the control input appears in the second equation of Eq. 20 and both uncertainties also appear only in this equation.

To demonstrate the implementation of the monitoring scheme, the reactor is initialized in mode 1, and it can be seen from Figures 3a–3c that the controller robustly stabilizes the reactant concentration and reactor temperature very quickly near the desired equilibrium point (asymptotic stability cannot be achieved because the existence of nonvanishing uncertainties perturbs the equilibrium point of the uncertain system to a new location in the vicinity of the nominal one). Figure 3d is a plot of the residual signals for the three mode observers. As shown in the figure, for $0 \leq t < 12.5$ h, the residual for mode observer 1 converges quickly to zero, whereas the residuals for the other mode observers exhibit a nonzero offset, which indicates that mode 1 is active during this time interval. As mode 1 is active, the value of V_1 is monitored to determine the operational health of the process. At $t = 0.4$ h, when the state is still outside the terminal set, V_1 starts to increase until $t = 0.5$ h (see Figure 4a), which implies that a destabilizing fault (all actuator faults in this section are simulated by abrupt faults that cancel out the control action u_i) occurs at $t = 0.4$ h and lasts for 0.1 h. At $t = 12.5$ h, a mode transition is triggered and detected as the residual of mode observer 1 jumps to a nonzero value. At this time, the residual of mode observer 2 becomes zero indicating that reactor operation has been switched to mode 2. Note that because the eigenvalues of L_i are chosen to be

large in magnitude, the residual signals of the mode observers converge to zero very rapidly and thus time delays in identifying the active modes are negligible. Immediately after the new mode has been identified, the supervisor activates controller 2 and begins to monitor the evolution of the value of V_2. At $t = 17.5$ h, the value of V_2 exceeds the specified threshold (see Figure 4b) indicating that the process state has escaped the terminal set of this mode (see also Figure 3), and that a fault has occurred. The fault lasts for 0.2 h and is then eliminated by activating a new backup configuration of actuators. Following recovery from the fault, the controller forces the state back into the terminal set as can be seen from Figures 4b and 3. Note that both state variables, as well as the residuals for mode observers 1 and 3, are influenced by the fault. However, the residual of mode observer 2 does not sense this fault because by design the residual for the active mode is insensitive to faults and uncertainties. In this manner, the local fault within mode 2 cannot be mistaken for a mode transition. At $t = 25$ h, another mode transition takes place and mode 1 is activated for a second time as can be deduced from the residual profiles in Figure 3d.

As indicated by its residual profile, mode 1 remains active until $t = 37.5$ h at which time the residual r_1 exhibits an offset while r_2 converges to zero, thus implying that mode 2 has become active. Mode 2 remains active until $t = 50$ h. During this time period, by monitoring V_2, we see that its value breaches the specified threshold at $t = 42.5$ h, which indicates that a fault has occurred. On the last time interval, for $t \geq 50$ h, the residual for mode observer 3 converges to zero indicating that mode 3 is active for all future times. Also, another fault appears at $t = 55$ h and lasts for 0.5 h as indicated by the profile of V_3 breaching its threshold. It can be seen from the simulation results that the proposed monitoring scheme can reliably detect and distinguish between mode transitions and faults.

To evaluate the monitoring performance of the proposed methodology in cases where measurement noise is present, white noises of magnitudes 0.01 kmol/m^3 and 1 K are added into the measurements of C_A and T, respectively. To accommodate the effects of noise, the thresholds for the mode observer residuals and fault detection schemes are relaxed. As can be seen from Figure 5, mode identification and fault detection can still be performed satisfactorily in the presence of measurement noise.

Finally, to illustrate the efficacy of the fault detection scheme under multiple actuator faults, we consider another scenario where two manipulated inputs are used to control the process. Specifically, the reactor is initialized at $(C_A, T) = (4.598$ kmol/m^3, 388.57 K) and remains in mode 1 for 2 h, and the inlet temperature for the first feed stream T_{A1} is used as an additional manipulated input, i.e., $u_1^1 = Q - Q_1^{\text{nom}}$ and $u_1^2 = T_{A1} - T_{A1}^{\text{nom}}$, where T_{A1}^{nom} is the nominal value of T_{A1} (all values used in this simulation scenario are the same as those used in the previous scenario). The process is subject to parametric uncertainty in the enthalpy of the reaction. Figure 6 shows that the controller is able to quickly stabilize the reactor around the desired steady state. At $t = 0.15$ h, both actuators start to malfunction, and as a result the value of the Lyapunov function V_1 (see Figure 6f) begins to increase immediately, breaching the specified threshold after 0.02 h at which time the faults are declared. At $t = 0.2$ h, a new backup configuration of actuators is activated and the faults are thus eliminated; consequently, the controller is able to restore stability and V_1 begins to decrease and falls below the specified threshold. The profiles of the residuals in Figure 6e show that the mode identification scheme is still capable of identifying the active mode in a timely fashion regardless of the uncertainty and the simultaneous faults.

Conclusions

In this work, a model-based framework for fault detection and monitoring of nonlinear hybrid process systems with control actuator faults and uncertain mode transitions was presented. The key idea was to design the mode observers such that they are able to work without information from the controller. Initially, a family of feedback controllers that enforce practical closed-loop stability and guarantee an arbitrary degree of uncertainty attenuation were designed. The performance of each fault-free closed-loop subsystem was explicitly characterized and used to derive rules and alarm thresholds for the detection of faults within each mode. To determine which mode is active at any given time and detect possible transitions between the constituent modes, a bank of dedicated mode observers were synthesized and run in parallel to the process. Using ideas from unknown input observer theory, the observers were designed to create a certain residual pattern in which only the residual of the mode observer for the active mode converges to the origin, thus allowing the reliable identification of the active mode irrespective of the faults and other uncertainties. Finally, the theoretical results were illustrated using a simulation example involving a chemical reactor that switches between multiple operating modes.

Literature Cited

1. Himmelblau DM. *Fault Detection and Diagnosis in Chemical and Petrochemical Processes*. New York: Elsevier Scientific Pub. Co., 1978.
2. Frank PM. Fault diagnosis in dynamic systems using analytical and knowledge-based redundancy — a survey and some new results. *Automatica*. 1990;26:459–474.
3. Basila M, Stefanek G, Cinar A. A model-object based supervisory expert system for fault tolerant chemical reactor control. *Comput Chem Eng*. 1990;14:551–560.
4. Kresta JV, Macgregor JF, Marlin TE. Multivariate statistical monitoring of process operating performance. *Can J Chem Eng*. 1991;69:35–47.
5. Huang B. Detection of abrupt changes of total least squares models and application in fault detection. *IEEE Trans Control Syst Techol* 2001;9:357–367.
6. Simani S, Fantuzzi C, Patton RJ. *Model-based Fault Diagnosis in Dynamic Systems Using Identification Techniques*. London: Springer, 2003.
7. Mhaskar P, McFall C, Gani A, Christofides PD, Davis JF. Isolation and handling of actuator faults in nonlinear systems. *Automatica*. 2008;44:53–62.
8. Armaou A, Demetriou M. Robust detection and accommodation of incipient component faults in nonlinear distributed processes. *AIChE J*. 2008;54:2651–2662.
9. Ghantasala S, El-Farra NH. Robust actuator fault isolation and management in constrained uncertain parabolic PDE systems. *Automatica*. 2009;45:2368–2373.
10. Yamalidou EC, Kantor J. Modeling and optimal control of discrete-event chemical processes using Petri nets. *Comput Chem Eng*. 1990;15:503–519.

11. Barton PI, Pantelides CC. Modeling of combined discrete/continuous processes. *AIChE J*. 1994;40:966–979.
12. Lee CK, Barton PI. Global optimization of linear hybrid systems with varying transition times. *SIAM J Control Optim*. 2008;47:791–816.
13. Branicky MS. Multiple Lyapunov functions and other analysis tools for switched and hybrid systems. *IEEE Trans Automat Control* 1998;43:475–482.
14. Liberzon D, Morse A. Basic problems in stability and design of switched systems. *IEEE Control Syst Mag*. 1999;19:59–70.
15. Decarlo RA, Branicky MS, Pettersson S, Lennartson B. Perspectives and results on the stability and stabilizability of hybrid systems. *Proc IEEE*. 2000;88:1069–1082.
16. Hespanha JP. Uniform stability of switched linear systems: extensions of Lasalle's invariance principle. *IEEE Trans Automat Control* 2004;49:470–482.
17. Bemporad A, Morari M. Control of systems integrating logic, dynamics and constraints. *Automatica*. 1999;35:407–427.
18. Hu B, Xu X, Antsaklis PJ, Michel AN. Robust stabilizing control law for a class of second-order switched systems. *Syst Control Lett*. 1999;38:197–207.
19. El-Farra NH, Christofides PD. Coordinating feedback and switching for control of hybrid non-linear processes. *AIChE J*. 2003;49:2079–2098.
20. Mhaskar P, El-Farra NH, Christofides PD. Predictive control of switched nonlinear systems with scheduled mode transitions. *IEEE Trans Automat Control* 2005;5:1670–1680.
21. El-Farra NH, Mhaskar P, Christofides PD. Output feedback control of switched nonlinear systems using multiple Lyapunov functions. *Syst Control Lett*. 2005;54:1163–1182.
22. Christofides PD, El-Farra NH. *Control of Nonlinear and Hybrid Process Systems: Designs for Uncertainty, Constraints and Time-Delays*. Berlin/Heidelberg: Springer-Verlag, 2005.
23. Balluchi A, Benvenuti L, Di Benedetto MD, Sangiovanni-Vincentelli AL. Design of observers for hybrid systems. In: Tomlin CJ, Greenstreet MR, editors. *Hybrid Systems: Computation and Control*. Berlin/Heidelberg: Springer-Verlag, 2002:76–89.
24. Alessandri A, Baglietto M, Battistelli G. Luenberger observers for switching discrete-time linear systems. *Int J Control* 2007;80:1931–1943.
25. Wang W, Zhou DH, Li Z. Robust state estimation and fault diagnosis for uncertain hybrid systems. *Nonlinear Anal* 2006;65:2193–2215.
26. Zhao F, Koutsoukos X, Haussecker H, Reich J, Cheung P. Monitoring and fault diagnosis of hybrid systems. *IEEE Trans Syst Man Cybern Part B-Cybern*. 2005;35:1225–1240.
27. Basseville M, Benveniste A, Tromp L. Diagnosing hybrid dynamical systems: fault graphs, statistical residuals and viterbi algorithms. In: *Proceedings of 37th IEEE Conference on Decision and Control*, Tampa, FL, 1998:3757–3762.
28. Narasimhan S, Biswas G. Model-based diagnosis of hybrid systems. *IEEE Trans Syst Man Cybern Part A-Syst Hum*. 2007;37:348–361.
29. Jin X, Huang B. Robust identification of piecewise/switching autoregressive exogenous process. *AIChE J*. 2010;56:1829–1844.
30. Sontag ED. Smooth stabilization implies coprime factorization. *IEEE Trans Automat Control* 1989;34:435–443.
31. Freeman RA, Kokotovic PV. *Robust Nonlinear Control Design: State-Space and Lyapunov Techniques*. Boston: Birkhauser, 1996.
32. Krstic M, Deng H. *Stabilization of Nonlinear Uncertain Systems*, 1st ed. Berlin: Springer, 1998.
33. Frank PM, Schrier G, Alcorta-García E. Nonlinear observers for fault detection and isolation. In: Nijmeijer H, Fossen TI, editors. *New Directions in Nonlinear Observer Design*. Berlin/Heidelberg: Springer-Verlag, 1999:399–422.

Appendix A: Proof of Theorem 1

Proof. As mode ε is active, by calculating the time derivative of the i-th residual $\dot{r}_i = \dot{x}_i - \dot{\xi}_i$ where $\dot{x}_i$ and $\dot{\xi}_i$ are given by Eqs. 1 and 8, respectively, it can be shown that the evolution of r_i is governed by

$$\begin{aligned}\dot{r}_i = {} & L_i r_i + (I - H_i C)[f_\varepsilon(x) - f_i(\xi_i)] \\ & + [(I - H_i C)A_\varepsilon - L_i(I - H_i C) - K_i C]x \\ & + (I - H_i C)[B_\varepsilon(u_\varepsilon + f_{a\varepsilon}) + W_\varepsilon(x)\theta_\varepsilon]\end{aligned}$$

Therefore, when Eqs. 9–12 are satisfied for all $i \in \mathcal{I}$, for residual r_ε that corresponds to the active mode, we have

$$\dot{r}_\varepsilon = L_\varepsilon r_\varepsilon + (I - H_\varepsilon C)[f_\varepsilon(x) - f_\varepsilon(\xi_\varepsilon)]$$

and for residual r_j, where $j \in \mathcal{I} - \{\varepsilon\}$, we have

$$\begin{aligned}\dot{r}_j = {} & L_j r_j + (I - H_j C)[(A_\varepsilon - A_j)x + f_\varepsilon(x) - f_j(\xi_j)] \\ & + (I - H_j C)[B_\varepsilon(u_\varepsilon + f_{a\varepsilon}) + W_\varepsilon(x)\theta_\varepsilon]\end{aligned}$$

which completes the proof of the theorem.

Appendix B: Proof of Proposition 2

Proof. L_ε being a Hurwitz matrix implies that, for any positive definite matrix S_ε, there exists a positive definite matrix P_ε that satisfies the Lyapunov equation $L_\varepsilon^T P_\varepsilon + P_\varepsilon L_\varepsilon = -S_\varepsilon$. We apply Lyapunov's direct method to analyze the stability and consider the function $V_\varepsilon = r_\varepsilon^T P_\varepsilon r_\varepsilon$ as a Lyapunov function candidate for the system of Eq. 13. Computing the time derivative of V_ε along the trajectory of the system of Eq. 13 gives

$$\begin{aligned}\dot{V}_\varepsilon &= r_\varepsilon^T (L_\varepsilon^T P_\varepsilon + P_\varepsilon L_\varepsilon) r_\varepsilon \\ &\quad + 2 r_\varepsilon^T P_\varepsilon (I - H_\varepsilon C)[f_\varepsilon(x) - f_\varepsilon(\xi_\varepsilon)] \\ &= -r_\varepsilon^T S_\varepsilon r_\varepsilon + 2 r_\varepsilon^T P_\varepsilon (I - H_\varepsilon C)[f_\varepsilon(x) - f_\varepsilon(\xi_\varepsilon)] \\ &\le -\lambda_{\min}(S_\varepsilon)\|r_\varepsilon\|^2 + 2\|r_\varepsilon\|\|P_\varepsilon(I - H_\varepsilon C)\|\omega_\varepsilon\|r_\varepsilon\| \\ &= [-\lambda_{\min}(S_\varepsilon) + 2\omega_\varepsilon \sigma_{\max}(P_\varepsilon(I - H_\varepsilon C))]\|r_\varepsilon\|^2\end{aligned}$$

where $\lambda_{\min}(\cdot)$ denotes the smallest eigenvalue of a matrix and $\sigma_{\max}(\cdot)$ denotes the largest singular value of a matrix. Therefore, as long as $\lambda_{\min}(S_\varepsilon) > 2\omega_\varepsilon \sigma_{\max}(P_\varepsilon(I - H_\varepsilon C))$, $\dot{V}_\varepsilon$ is negative definite and thus, for the system of Eq. 13, the origin is asymptotically stable.

Manuscript received Jun. 3, 2010, and revision received Oct. 6, 2010.